01 Aug 2003

Quantifying the Effects on EMI and SI of Source Imbalances in Differential Signaling

Chen Wang

James L. Drewniak
Missouri University of Science and Technology, drewniak@mst.edu

Recommended Citation

C. Wang and J. L. Drewniak, "Quantifying the Effects on EMI and SI of Source Imbalances in Differential Signaling," *Proceedings of the IEEE International Symposium on Electromagnetic Compatibility (2003, Boston, MA)*, vol. 2, pp. 865-868, Institute of Electrical and Electronics Engineers (IEEE), Aug 2003.
The definitive version is available at https://doi.org/10.1109/ISEMC.2003.1236722

Quantifying the Effects on EMI and SI of Source Imbalances in Differential Signaling

Chen Wang
Electromagnetic Compatibility Laboratory
Dept. of Electrical and Computer Engineering
University of MO – Rolla
Rolla, MO 65409
cwang@umr.edu

James L. Drewniak
Electromagnetic Compatibility Laboratory
Dept. of Electrical and Computer Engineering
University of MO – Rolla
Rolla, MO 65409
drewniak@ece.umr.edu

Abstract

Imbalances in differential signaling can introduce common-mode components, resulting in signal integrity (SI) problems as well as EMI problems. Three-port mixed-mode S-parameters are employed to quantify the impacts on EMI. The EMI problems caused by delay skew and slew rate skew are investigated.

Keywords

Differential signaling, delay skews, slew rate skews, imbalances, EMI, SI.

INTRODUCTION

Differential signals are widely used in digital circuits because of the rejection of common-mode noise, as well as the reduction of EMI levels. However, imbalances in differential signals will degrade the performance. Imbalances may be caused by skew in differential sources, different lengths in the two lines of the differential pair, routing differential lines through a pin field, layer transitions of differential lines with vias, and imbalances at terminations, etc.

Since imbalances in differential signaling are inevitable, quantifying the effects of the imbalances on both SI and EMI is essential in the design of differential lines. A few issues should be addressed: how does skew in a differential source influence the level of EMI and the quality of signals; how much length difference between the two differential traces can be tolerated; how much skew is introduced at via transitions, etc. This work quantifies the impact of skew from differential sources on EMI levels.

QUANTIFYING THE EFFECTS OF THE IMBALANCED DIFFERENTIAL SOURCES ON EMI

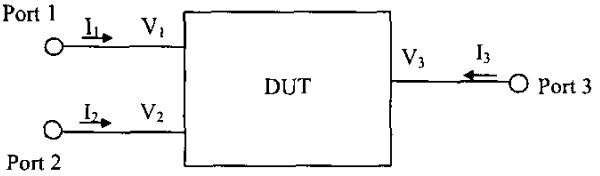

Figure 1. A general 3-port network.

A three-port network is shown in Figure 1. Port 1 and Port 2 are paired as a differential port. Port 3 is a single-ended port. The single-ended port can be the common-mode current on differential lines (e.g., as measured with a clamp on current probe), the near field of the circuits, or the far field radiation, etc. The differential and common-mode voltages and currents can be defined as [1],

$$V_{dm} \equiv V_1 - V_2,\ V_{cm} \equiv \frac{1}{2}(V_1 + V_2), \tag{1}$$

$$I_{dm} \equiv \frac{1}{2}(I_1 - I_2),\ I_{cm} \equiv I_1 + I_2, \tag{2}$$

where V_1, V_2, I_1 and I_2 are the voltages and currents at Port 1 and Port 2, respectively. The incident and reflected differential and common-mode waves can be written as [1]

$$a_{dm} \equiv \frac{1}{\sqrt{2}}(a_1 - a_2),\ a_{cm} \equiv \frac{1}{\sqrt{2}}(a_1 + a_2), \tag{3}$$

$$b_{dm} \equiv \frac{1}{\sqrt{2}}(b_1 - b_2),\ b_{cm} \equiv \frac{1}{\sqrt{2}}(b_1 + b_2), \tag{4}$$

where a_1, a_2, b_1 and b_2 are the incident and reflected waves at Port 1 and Port 2, respectively. Therefore, the 3-port network can be represented in terms of mixed-mode S-parameters by

$$\begin{bmatrix} b_{dm} \\ b_{cm} \\ b_s \end{bmatrix} = \begin{bmatrix} S_{dd} & S_{dc} & S_{ds} \\ S_{cd} & S_{cc} & S_{cs} \\ S_{sd} & S_{sc} & S_{ss} \end{bmatrix} \begin{bmatrix} a_{dm} \\ a_{cm} \\ a_s \end{bmatrix}, \tag{5}$$

where $a_s = a_3$ and $b_s = b_3$ are the incident and reflected waves at Port 3, respectively. Then the relationship between the mixed-mode S-parameters and the conventional S-parameters can be found as

$$\begin{bmatrix} S_{dd} & S_{dc} & S_{ds} \\ S_{cd} & S_{cc} & S_{cs} \\ S_{sd} & S_{sc} & S_{ss} \end{bmatrix} = T \cdot \begin{bmatrix} S_{11} & S_{12} & S_{13} \\ S_{21} & S_{22} & S_{23} \\ S_{31} & S_{32} & S_{33} \end{bmatrix} \cdot T^{-1}, \tag{6}$$

where

$$T = \begin{bmatrix} \frac{1}{\sqrt{2}} & -\frac{1}{\sqrt{2}} & 0 \\ \frac{1}{\sqrt{2}} & \frac{1}{\sqrt{2}} & 0 \\ 0 & 0 & 1 \end{bmatrix}.$$

If Port 3 characterizes the radiation, S_{sd} in (5) quantifies the radiation from a pure differential excitation (two sources equal in magnitude but out of phase), and S_{sc} quantifies the radiation from a pure common-mode excitation (two sources equal in magnitude and in phase).

0-7803-7835-0/03/$17.00 © 2003 IEEE

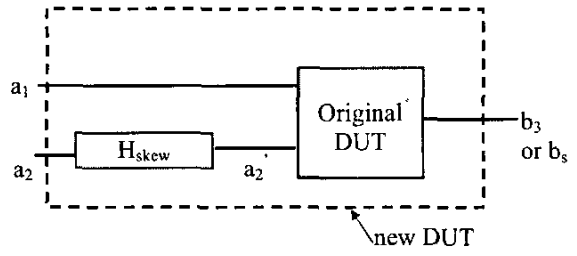

Figure 2. A 3-port network including the imbalances of a differential source.

In most cases where differential signaling reduces EMI levels, the radiation from the differential excitation should be less than that from the common-mode excitation, that is $|S_{sd}| < |S_{sc}|$. However, practical differential excitation cannot be perfect. Invariably, it consists of both a pure differential component and a pure common-mode component. For a linear system, the radiation from the differential circuit driven by a differential source with skew can be quantified as a linear combination of S_{sd} and S_{sc}, as detailed below.

In Figure 2, the original DUT (Device Under Test) is presumed to be a differential signaling system, with a_2 and a_1 acting as an ideal differential source pair ($a_2 = -a_1$). Because there is some skew in the excitation of the differential system, the actual excitation are a_1 and a_2', where a_2' is related to a_2 and a_1 by H_{skew}, with

$$H_{skew} = \frac{a_2'}{a_2} = -\frac{a_2'}{a_1}. \quad (7)$$

Therefore, the excitation pair (a_1 , a_2') consists of the differential component a_{dm} and a common-mode component a_{cm}, where

$$a_{dm} = \frac{1}{\sqrt{2}} a_1 (1 + H_{skew}) \quad (8)$$

$$\text{and } a_{cm} = \frac{1}{\sqrt{2}} a_1 (1 - H_{skew}). \quad (9)$$

Since the DUT is a linear system, superposition can be applied to obtain the b_s,

$$b_s = S_{sd} \times a_{dm} + S_{sc} \times a_{cm}$$
$$= \frac{1}{\sqrt{2}} [S_{sd} \times (1 + H_{skew}) + S_{sc} \times (1 - H_{skew})] a_1, \quad (10)$$

where S_{sd} and S_{sc} are the mixed-mode S-parameters of the original DUT. In order to quantify the effects of imbalanced differential sources, the excitation is viewed as ideal (a_1 and a_2), and the transfer function H_{skew} is integrated into the original DUT to form a new DUT. Then the S_{sd} of the new DUT ($S_{sd\text{-}new}$) can be obtained as

$$S_{sd-new} = \frac{1}{2} [S_{sd} \times (1 + H_{skew}) + S_{sc} \times (1 - H_{skew})]. \quad (11)$$

The S-parameter $S_{sd\text{-}new}$ characterizes the overall radiation characteristics, including the radiation characteristics of the original DUT and the impact of the unbalanced excitations.

MEASUREMENTS AND NUMERICAL MODELING RESULTS

Measurements and numerical modeling tools were employed to verify the analysis in the previous section. The measurement configuration is shown in Figure 3. A pair of differential microstrip traces was routed across a complete gap in the PCB ground plane. The traces were connected to Port 2 and Port 4 of a 4-port network analyzer through two 0.85" semi-rigid coaxial cables. Port 2 and Port 4 were paired as one balanced port. The PCB ground plane was attached to a 60 cm × 60 cm aluminum plate using copper tape. The aluminum plate reduced the coupling from the DUT to the measurement system so that the experiment was more repeatable. Port 1 of the network analyzer, as a single-ended port, was connected to a 3" long monopole sensing probe with a diameter of 30 mils. The conventional S-parameters were measured and were converted to the mixed-mode S-parameters using equation (6).

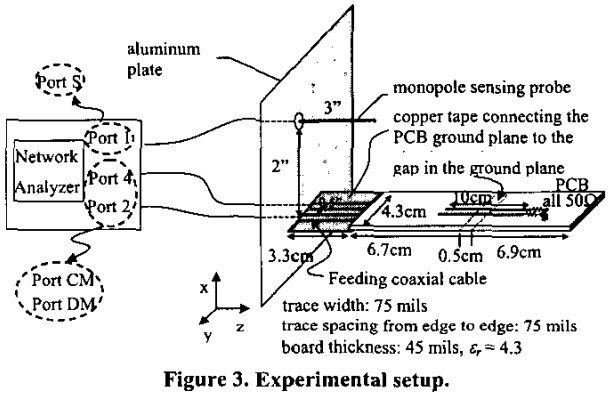

Figure 3. Experimental setup.

FDTD was employed to model the experimental configuration shown in Figure 3. Though the measured mixed-mode S-parameters, specifically S_{sd} and S_{sc}, were obtained from converting the conventional S-parameters, S_{sd} and S_{sc} in the FDTD modeling were obtained with a pure differential excitation and a pure common-mode excitation, respectively. A comparison between the FDTD results and the measurements is shown in Figure 4. The agreement for the common-mode excitation is very good (within 3 dB) over the entire frequency range of interest (from 1 MHz to 10 GHz). The results of the differential mode excitation are very sensitive to the degree of the balance of the configuration, because any imbalances will introduce a common-mode component. Since S_{sc} is much larger than S_{sd}, even a small amount of common-mode component in the circuit will increase the radiation dramatically. Agreement for the pure differential-mode excitation is good up to 7 GHz. The discrepancy for differential mode excitation at high frequencies is partly due to the difficulty in constructing perfectly balanced configurations, including balanced feed cables, balanced soldering etc. Any imbalance introduced

to the configuration with the differential excitation will influence the measurement.

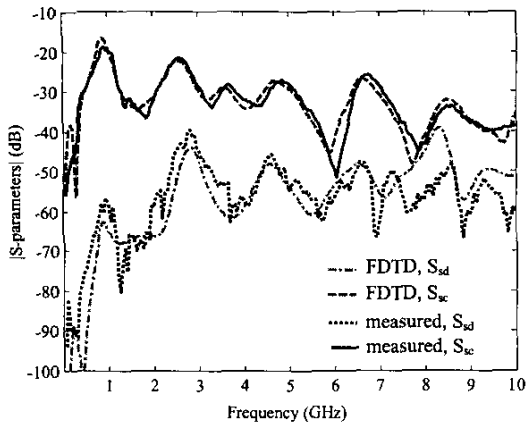

Figure 4. Comparison of FDTD and measured results.

Agreements between the measured and modeled results indicate that the FDTD modeling is valid. While arbitrary skew is not easily added in the experiment, they can be added in the FDTD modeling. Therefore, the FDTD approach is applied to investigate the effects of imbalanced differential sources on EMI. Two cases are studied below: delay skew and slew rate skew.

A. Delay Skew

Referring to Figure 2, suppose there is a delay skew t_0 between a_1 and a_2', i.e., $a_2'(t) = -a_1(t-t_0)$. In the frequency domain, this delay skew corresponds to a phase shift of $e^{-j\omega t_0}$. Therefore, $H_{skew}(\omega) = e^{-j\omega t_0}$. According to (11),

$$S_{sd\_new} = \frac{1}{2}[S_{sd} \times (1 + e^{-j\omega t_0}) + S_{sc} \times (1 - e^{-j\omega t_0})]. \quad (12)$$

The same configuration shown in Figure 3 is used to verify (12). The results are shown in Figure 5. The dashed and the dark solid curves are S_{sc} and S_{sd} of the original DUT, respectively. The dotted curve is the result from (12) for $t_0 = 170\,ps$, and the gray solid curve is the result from the full wave FDTD modeling when the sources have a delay skew of 170 ps. As expected, they overlay each other exactly.

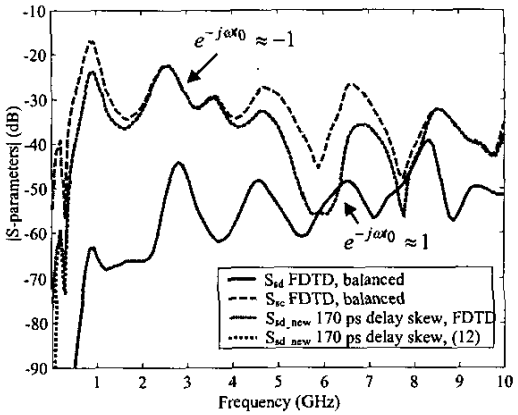

Figure 5. The effect of a delay skew on EMI

Equation (12) clearly indicates that the impact of a delay skew varies periodically with frequency. At frequencies where $e^{-j\omega t_0} \approx 1$, the delay skew does not have a significant impact. However, at frequencies where $e^{-j\omega t_0} \approx -1$, the excitations are actually common-mode due to the delay skew, therefore, the radiation increases to the level of a configuration with a common-mode feeding. As a practical engineering design guideline, the delay skew, t_0, should be small enough so that $e^{-j\omega t_0}$ is approximately 1 at frequencies where the harmonics of the circuit are significant.

B. Slew Rate Skew

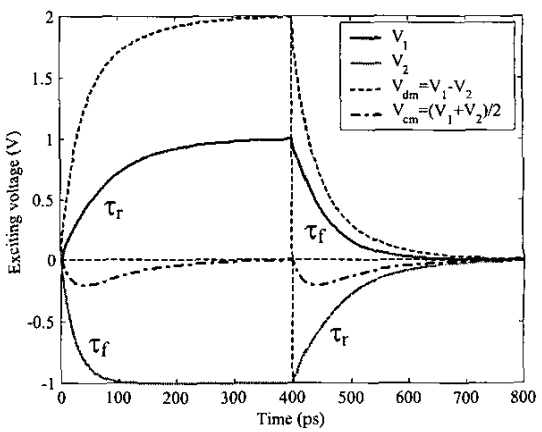

Figure 6. Waveforms of the input exponential pulses.

Referring to Figure 3, assume the input voltage sources are pulses with exponential rising and falling edges, as shown in Figure 6. The input voltage pulse V_1 can be expressed as

$$V_1 = \begin{cases} 1 - e^{-\frac{t}{\tau_r}} & 0 < t < t_1 \\ e^{-\frac{t-t_1}{\tau_f}} & t > t_1 \end{cases} \quad (13)$$

where τ_r and τ_f are the time constants of the rising and falling edges of V_1, respectively. The Fourier transform of (13) is

$$V_1(\omega) = -\frac{1}{j\omega}(e^{-j\omega t_1} - 1) + \frac{1}{1/\tau_r + j\omega}\left(e^{-(\frac{1}{\tau_r} + j\omega)t_1} - 1\right) + \frac{1}{1/\tau_f + j\omega}e^{-j\omega t_1} \quad (14)$$

If $\tau_f = \tau_r$, the differential excitation is perfectly balanced and the even harmonics are zero. However, in a real CMOS circuit, the falling time usually is not equal to the rising time, resulting in energy in V_1 and V_2 spreading into the even harmonics. From Figure 6, it can be observed that the fundamental frequency of the common-mode component, V_{cm} equals the first even harmonic of V_1 or V_2, while the even harmonics in the differential component V_{dm} are zero. Therefore, comparing to the perfectly balanced case ($\tau_f = \tau_r$), the radiation from the case with $\tau_f \neq \tau_r$ is expected to increase around the even harmonics provided the radiation from the common-mode excitation is dominant.

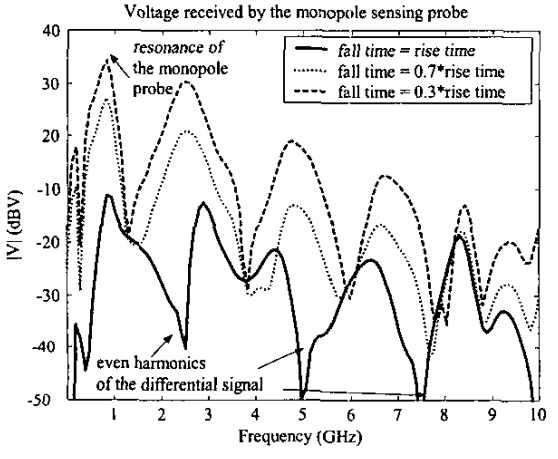

Figure 7. Radiation levels as a function of slew rate skew.

The geometry in Figure 3 is employed to verify the above conjecture. The voltage received by the monopole sensing probe is calculated with equation (10), where S_{sd} and S_{sc} are obtained from the FDTD simulations as described in previous section. The duration of the input pulses V_1 and V_2 is 800 ps, corresponding to a fundamental frequency of 1.25GHz. The time constant for the rising edge τ_r is fixed to 80 ps, the time constant for the falling edge τ_f is varied from 100%, 70% to 30% of τ_r. The results of the received voltage as a function of frequency are plotted in Figure 7, with each curve corresponding to a different value of τ_f. The peak around the 1 GHz is due to the resonance of the monopole sensing probe. While the radiation from the case with $\tau_f = \tau_r$ has nullss at the even harmonics 2.5 GHz, 5 GHz, 7.5 GHz, etc., the radiation from the cases with $\tau_f \neq \tau_r$ has peaks at these frequencies. Therefore, the slew rate skew will increase the EMI levels for a system where radiation from common-mode excitation is dominant. Peaks may appear at the even harmonics of V_1 or V_2.

CONCLUSIONS

The effects on radiation of imbalanced differential sources can be quantified using equation (11). The delay skew and the slew rate skew have been investigated. The impact of the delay skew will alternately change between common-mode excitation and differential mode excitation with the frequency. Slew rate skew will introduce even harmonics to the common-mode component, increasing the EMI level at these frequencies.

REFERENCES

[1] David E. Bockelman, William R. Eisenstadt, "Combined differential and common-mode scattering parameters: theory and simulation", *IEEE Trans. Microwave Theory Tech.*, vol. 43, pp. 1530-1539, July 1995.

[2] ____, "Pure-mode network analyzer for on-wafer measurements of mixed-mode s-parameters of differential circuits", *IEEE Trans. Microwave Theory Tech.*, vol. 45, pp. 1071-1077, July 1997.